Chapter 6

REFLECTION OF A SECOND SOUND

6.1 Introduction

In previous studies, there have been many experimental and theoretical studies on reflection of a second sound from a He II free surface as already described before. However, these previous theoretical values of the temperature amplitude reflection coefficient R_{22} of a second sound thermal pulse from a free surface are all somehow incorrect. In this thesis, the experimental value of R_{22} obtained by the direct measurement of the temperature amplitudes of an incident and reflected thermal pulses is compared with the correct theoretical value estimated from the most reliable kinetic theory result with the boundary condition where the enthalpy flux density of evaporated vapor is taken into account in the energy balance formular. Furthermore, the reflection coefficient $R_{22,rigid}$ of a second sound from a rigid wall is investigated for the comparison with the reflection coefficient R_{22} from a He II free surface.

6.2 General Boundary Condition of He II-Vapor Interface

General boundary condition for the liquid-vapor interface is given by Meinhold-Heerlein[30]. This boundary condition consists of the conserva-

tion laws of mass, momentum and energy and the entropy balance. The general fluxes for He II may be obtained from thermohydrodynamic theories. The most complete of them, which includes all the non-linear term and dissipative processes in He II, has been given by Khalatnikov[60]. According to this theory, the fluxes of mass, momentum and energy take the following forms:

(1) Mass

$$\rho\, v = \rho_v\, v_v = j, \tag{6.1}$$

(2) Momentum

$$\rho\, v^2 + \frac{\rho_s \rho_n}{\rho}\, v_{ns}^2 + P = \rho_v\, v_v^2 + P_v, \tag{6.2}$$

(3) Energy

$$j\left(h + \frac{1}{2}\, v^2\right) + \rho_s\, s\, T\, v_{ns} + \left(1 - \frac{1}{2}\frac{\rho_n}{\rho}\right)\, v_{ns}^2\, \rho_n\, v + \frac{\rho_s}{\rho}\left(v_{ns} v + \frac{\rho_s}{\rho}\, v_{ns}^2\right)\, \rho_n\, v_{ns} + J_Q = j\left(h_v + \frac{1}{2} v_v^2\right) + J_Q^v, \tag{6.3}$$

where the subscript v and the no subscript indicate the physical value in the vapor phase and that in the He II phase. h is the enthalpy per unit mass. J_Q is the irreversible part of the heat flux in the He II, which can be written as $J_Q = -\kappa\, \mathrm{grad}\, T$, where κ is the thermal conductivity of the normal fluid. Linearization of these equation for the momentum and the energy gives as

$$P = P_v, \tag{6.4}$$

$$j\, h + \rho_s\, s\, T\, v_{ns} + J_Q = j\, h_v + J_Q^v, \tag{6.5}$$

Eq. (6.5) can be simply written in the case of the equilibrium condition at the saturated vapor temperature T_0 as

$$j\, L_0 = \rho_s\, s\, T_0\, v_{ns} + J_Q - J_Q^v, \tag{6.6}$$

where L_0 is the latent heat of vaporization ($L_0 = h_{0,v} - h_0$, where $h_{0,v}$ and h_0 are the enthalpies of vapor and He II at the temperature T_0). Eq (6.6) is valid only in case the evaporated vapor flow is not occurred in the vapor phase. But, in previous theoretical studies, it is wrong that the boundary

condition of Eq. (6.6) is used in the estimation of the theoretical value of R_{22} because the evaporated vapor flow is caused in case the He II evaporation induced by a thermal pulse impingement as described in Chap. 4. Therefore, the boundary condition of Eq. (6.6) is modified in next Sec.

The boundary condition of Eq. (6.6) gives some physical insight into the process occurring at the free surface of He II. The first two terms on right-hand side of Eq. (6.6) represent the total heat flow in He II, which consists of the reversible part $\rho_s s T_0 v_{ns}$ and the irreversible part $J_Q = -\kappa \operatorname{gard} T$, and the third term the irreversible heat flow in the vapor $J_{Q,v} = -\kappa_v \operatorname{gard} T_v$, where κ_v is the thermal conductivity of vapor. Thus one may conclude from Eq. (6.6) that differences in the total heat flow in He II and vapor lead to an evaporation of He II. The boundary condition Eq. (6.6) also introduce why evaporation process are so important for He II. The reasons are that the reversible part of the heat flow is extremely high in He II and that the heat of vaporization is relatively small compared with other liquids. This implies that the evaporation mass flux j is high, even if only small deviations from the thermodynamic equilibrium appear in He II and caused heat fluxes.

In particular, this unusual property of He II can be made clear by comparing it with ordinal liquids. For such liquids, a formula similar to Eq. (6.6) is represented:

$$j L_0 = J_Q - J_Q^v, \tag{6.7}$$

In this special case, however, the reversible part of heat flux, which is characteristic for He II, is missing. Excluding the regions near the critical points, the heat conductivities of most of the classical liquids and gases, even if one considers liquid metals, are small and thus, as in acoustic phenomena, small deviations from equilibrium mostly give rise to negligible evaporation mass flux.

6.3 Reflection on He II Free Surface

6.3.1 Theoretical reflection coefficient

The theoretical R_{22} is derived through some modification to the previous theoretical studies[21], [22], [26], [27], [31]. In the present modified treatment the modification is made to the energy balance relation at the He II-vapor boundary. The enthalpy flux density of evaporated vapor is put into the balance relation. And the evaporation mass flux is correctly evaluated based on the kinetic theory result solved by Sone and Onishi[5]. The boundary condition of Eq. (6.6) can not be used in the case of the evaporated vapor flow is induced in the vapor phase. The correct energy flux density balance across a He II free surface is given by

$$W - w - q_{1st} = j_\infty L_0 + j_\infty h_\infty, \tag{6.8}$$

in the approximation where the kinetic energy term is neglected. Here j_∞ is the evaporation mass flux in the uniform flow region which is evaluated on the basis of the kinetic theory analysis result[5], and $j_\infty h_\infty$ is the enthalpy flux density of evaporated vapor, where h_∞ is the specific enthalpy of the uniform flow in the vapor expressed in terms of the specific heat of the vapor at constant pressure, $c_{P,v}$.

$$h_\infty = c_{P,v} T_\infty, \tag{6.9}$$

W is the impinging energy flux density brought by accompanying a second sound thermal pulse

$$W = \rho_0 c_P a_{20} \Delta T_i, \tag{6.10}$$

and w is the energy flux density carried away by a reflected second sound thermal pulse from the free surface

$$w = \rho_0 c_P a_{20} \Delta T_r, \tag{6.11}$$

and q_{1st} is the energy flux density brought by a first sound wave generated on the free surface which is given by the heat function $(c_p T_0)$ times v_n,

here v_n in the first sound can be derived from the substitution Eq. (2.41) that is eliminated the thermal expansion coefficient α_{exp} into Eq. (4.40).

$$q_{1st} = c_P\, T_0\, \Delta P_{1st}/a_{10}, \tag{6.12}$$

where ΔP_{1st} and a_{10} are the pressure rise of the first sound which is approximated by the pressure rise of evaporation wave ΔP_e in the present experimental situation and the speed of first sound. The term of q_{1st} was ignored in the theoretical estimation of R_{22} by Hunter and Osborne[21], through it was taken into account in the paper of R_{22} estimated by Chernikova-Khalatnikov[28][61] and Wiechert and Buchholz[31]. In the present treatment, it is found that q_{1st} can not be ignored near the λ point because the specific heat c_P becomes extremely large near the λ point. The temperature boundary condition on the free surface, Eq. (4.1), is rewritten in terms of R_{22} as

$$\Delta T_W = \Delta T_i + \Delta T_r = (1 + R_{22})\Delta T_i. \tag{6.13}$$

It is already experimentally confirmed, as shown in Figs. 4.2 and 4.6, that Eq. (4.1) is valid. Substituting Eqs. (4.4), (4.5), (4.10), (4.11), (4.14), and (6.9) through (6.13) into (6.8), the following relation among ΔT_W, v_∞, α_c and R_{22} is given as

$$\begin{aligned}
&\rho_0\, c_P\, a_{20} \Delta T_W \frac{1 - R_{22}}{1 + R_{22}} \\
&- \frac{c_P\, T_0\, P_0}{a_{10}} \left\{ \exp\left(\frac{L_0}{RT_0} \frac{\Delta T_W}{T_W} \right) \left(1 + C_4^{**} \frac{v_\infty}{\sqrt{2RT_W}} \right) - 1 \right\} \\
&- \frac{P_0 \exp\left(\frac{L_0}{RT_0} \frac{\Delta T_W}{T_W} \right) \left(1 + C_4^{**} \frac{v_\infty}{\sqrt{2RT_W}} \right) v_\infty}{RT_W \left(1 + d_4^* \frac{v_\infty}{\sqrt{2RT_W}} \right)} \\
&\times \left\{ L_0 + c_{P,v}\, T_W \left(1 + d_4^* \frac{v_\infty}{\sqrt{2RT_W}} \right) \right\} = 0,
\end{aligned} \tag{6.14}$$

where $T_W = \Delta T_W + T_0$ and $C_4^{**} = C_4^* - 2\sqrt{\pi}\frac{1-\alpha_c}{\alpha_c}$. In order to estimate the theoretical value of R_{22} from Eq. (6.14), another relation among ΔT_W, α_c

and v_∞ must be given. This relation are given by Eq. (4.16). The theoretical value of R_{22} is numerically given by Eqs. (4.16) and (6.14). For a specified value of α_c, the particle velocity v_∞ is numerically given by Eq. (4.16) for small values of ΔT_W. The theoretical value of R_{22} is numerically solved from Eq. (6.14) for a set of parameters, v_∞, ΔT_W and α_c. The theoretical value of R_{22} is independent of ΔT_W as far as ΔT_W is small, because the linear approximation is applied in the present treatment. All the physical quantities required in the calculation are computed with the aid of the thermo-physical properties software, HEPAK (CRYODATA INC.).

6.3.2 Comparison of experimental result with theoretical value of R_{22}

The temperature amplitude reflection coefficient R_{22} of a thermal pulse at a He II-vapor interface is obtained by the direct measurement of the temperature rises of an incident and a reflected thermal pulses with the superconductive temperature sensor. The result, indicated by solid circles, is presented in Fig. 6.1. The present experimental result is found to agree quite well with the previous experimental results[21], [25], [33] that are not presented in Fig. 6.1. The broken line indicates the Chernikova theory[28], which is sometimes referred to as the Khalatnikov theory[61]. The detail of the Chernikova-Khalatnikov theory is described in Appendix B. It is evident that the present experimental result largely deviates from the Chernikova-Khalatnikov theory. The theory which is a kind of an equilibrium theory takes no account of the slip boundary condition at a phase surface which should be derived from the kinetic theory analysis. The solid and dotted lines indicate the theoretical R_{22} for the cases of $\alpha_c = 1.0$ and 0.6 derived through some modification as mentioned in Sec. 6.3.1. It is seen that the experimental data points lie between the lines for $\alpha_c = 0.6$ and for 1.0 except at the temperatures very close to the λ temperature.

The open circles indicate the values of R_{22} that is converted from the condensation coefficients obtained experimentally through the same estimation procedure described above. The agreement between the di-

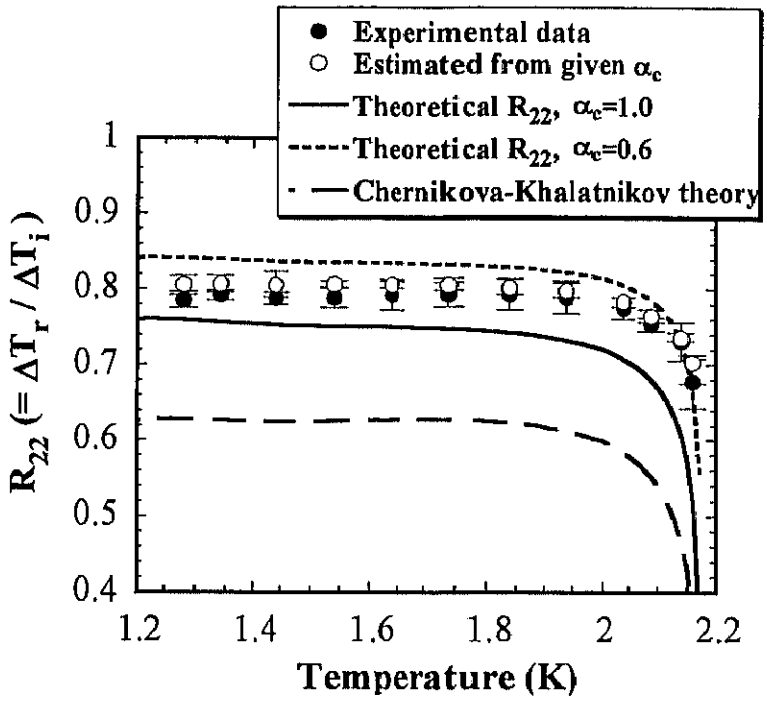

Fig. 6.1: The temperature amplitude reflection coefficient R_{22} of a thermal pulse at a He II free surface as a function of temperature. The experimental data are shown by solid circles. The open circles indicate the reflection coefficient R_{22} converted from the condensation coefficient α_c obtained experimentally. The solid and the dotted lines are the theoretical results presented in the text for $\alpha_c = 1.0$ and 0.6. The broken line is the Chernikova-Khalatnikov theory.

rect measurement result indicated by solid circles and that converted from the condensation coefficient indicated by open circles is fairy good. The satisfactory agreement between data obtained in the two independent measurements indicates the both measurements of α_c and R_{22} are valid.

6.4 Reflection on Rigid Wall

The reflection of a second sound from a rigid wall is investigated for the comparison with the reflection from a He II free surface. The temperature amplitude reflection coefficient of a second sound from the top plate of the experimental cell is measured with a wall mount type superconductive

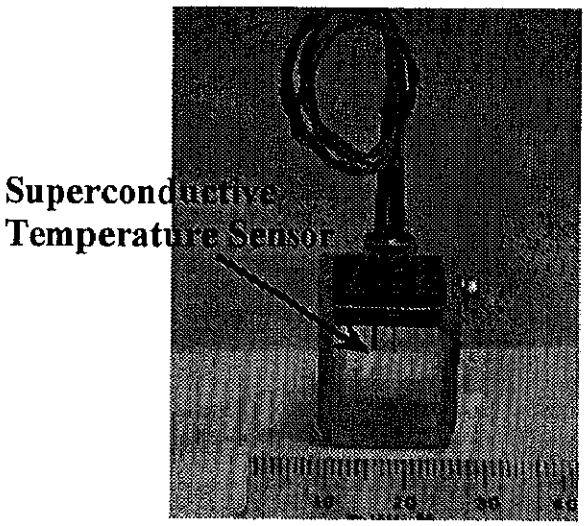

Fig. 6.2: The picture of the experimental cell for the reflection experiment of a second sound from a rigid wall.

temperature sensor. In addition to the temperature measurement, the reflection process is also visualized with a laser holographic interferometer.

6.4.1 Experimental setup

The experimental setup of this temperature measurement study is same setup of the evaporation experiment except a experimental cell. The experimental cell is a rectangular solid, a width of $15\,mm$, a height of $17\,mm$ and a length of $15\,mm$. The cell is composed of four acrylic resin side walls and an adiabatic top plate of Bakelite as shown in Fig. 6.2. A planar Nichrom thin film heater is located at the bottom of the cell. The superconductive temperature sensor is mounted on the top plate of the experimental cell as indicated in Fig. 6.2, the location of the sensing element is about $6\,mm$ from the top plate. And the experimental cell for the visualization of this reflection study is same cell for the evaporation experiment.

6.4.2 Visualization

The interferogram visualization result of the reflection of a second sound thermal pulse from a rigid wall are shown in Fig. 6.3.b. The interferogram shown in Fig. 6.3.b is taken in the finite-fringe mode. The experiment conditions, $T_0 = 1.74\,K$, $q = 25\,W/cm^2$ and $t_H = 200\,\mu s$ is same condition of Fig. 4.2.b. The x-t diagram for the process corresponding to Fig. 6.3.b which was taken at $t_D = 2.0\,ms$ after the thermal pulse generated from a heater is drawn in Fig. 6.3.a, where t_D is the time interval from the thermal pulse generated to photographing. First a thermal pulse

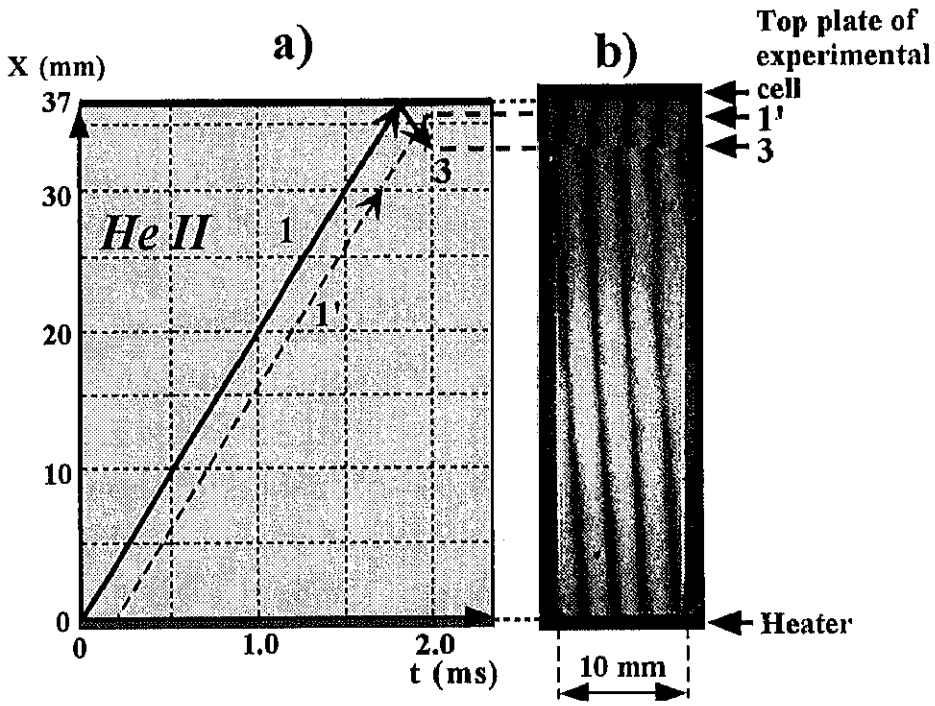

Fig. 6.3: The x-t diagram and the finite-fringe interferogram of the reflection of a second sound thermal pulse from a rigid wall of the top plate. 1: the impinging thermal pulse front, 3: the reflected thermal pulse front, 1′: the impinging thermal pulse tail. a): the x-t diagram for the reflection of a thermal pulse. Solid and broken arrows indicate wave front and tail. b): the finite-fringe interferogram showing the thermal pulse. $T_0 = 1.74\,K$, $q = 25\,W/cm^2$, $t_H = 200\,\mu s$, $t_D = 2.0\,ms$, where t_D is the duration time after the thermal pulse generated from a heater to photographing.

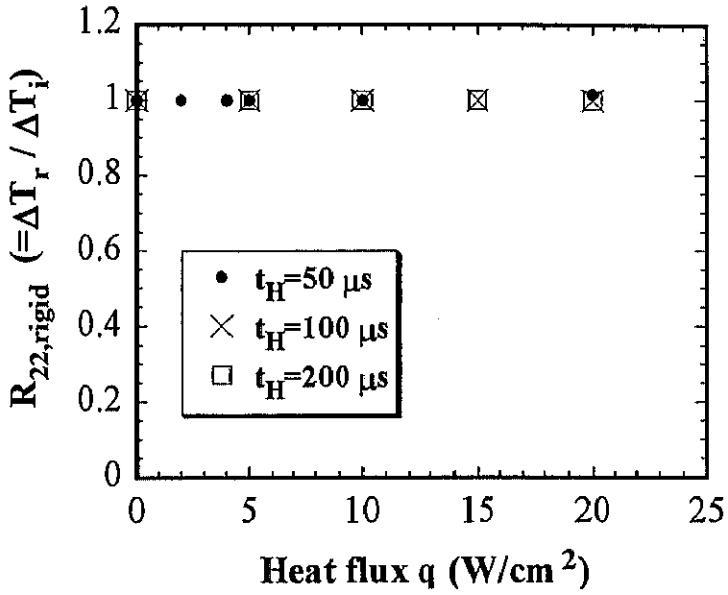

Fig. 6.4: The temperature amplitude reflection coefficient $R_{22,rigid}$ of a thermal pulse from a rigid wall as a function of heat flux q. $T_0 = 1.74\,K$, $t_H = 50$, 100, $200\,\mu s$.

emitted from the heater propagates upward through He II nearly at the speed of second sound ($20\,m/s$) as indicated by the *arrow* 1, the thermal pulse impinges onto the rigid wall of top plate. At the same time, the impinging thermal pulse is reflected from the top plate propagating downward through He II (*arrow* 3). In Fig. 6.3.b, it is seen that a thermal pulse does not change the sign of the temperature variation upon reflection from a rigid wall and thus the reflected and impinging thermal pulses overlap each other adjacent to a rigid wall. And the formation of a thermal shock is clearly recognized at the reflected thermal pulse front in the picture, in which the thermal shock front is indicated by the *arrow* 3. Next, the temperature amplitude reflection coefficient $R_{22,rigid}$ of the thermal pulse is investigated in next Sec.

6.4.3 Reflection coefficient

The temperature amplitude reflection coefficient $R_{22,rigid}$ of a thermal pulse from a rigid wall is measured with a wall mount type superconductive

temperature sensor. The reflection coefficient of a thermal pulse from a rigid wall as a function of heat flux q is indicated in Fig. 6.4. It is found that the reflection coefficient of the thermal pulse from the rigid wall is unity and that this reflection coefficient is not changed by the differences of the heat flux q and the heating time t_H. This unity means that the energy in the thermal pulse is not used in the case of the reflection from the rigid wall. For another temperature $T_0 = 1.84$ and $1.94\,K$, it is also confirmed that the reflection coefficient is unity. $R_{22,rigid} = 1$ also verifies that the temperature measurement with a superconductive temperature sensor is valid in the present experiment.

It is already indicated in Fig. 6.1 that the temperature amplitude reflection coefficient R_{22} of a second sound from a free surface is about 0.8 except near the λ point, and R_{22} is decreased as the temperature approaches to λ point. On the other hand, it is expected that the reflection coefficient $R_{22,rigid}$ from the rigid wall is unity even if the temperature approaches to λ point. It is considered for this reason that the energy flux density that is applied by an impinging thermal pulse onto a He II free surface is decreased, if it is compared at the same condition of T_W, because the speed of second sound is decreased as the temperature approaches to λ point, though the energy flux density used for evaporation within the applied energy flux density is not decreased as the temperature approaches to λ point.

6.5 Concluding Remarks

The reflection of a second sound thermal pulse from both a He II free surface and a rigid wall is experimentally investigated, and following conclusions are drawn.

1. It is pointed out that the previous theoretical R_{22} studies[21], [22], [26], [27], [28], [31] are all somehow incorrect . The correct theoretical R_{22} is derived through some modification to the previous theoretical studies. In the present modified treatment the modification is made to

the energy balance relation at the He II-vapor boundary. The enthalpy flux density of evaporated vapor is put into the balance relation. And the evaporation mass flux is correctly evaluated based on the kinetic theory result solved by Sone and Onishi[5].

2. The temperature amplitude reflection coefficient R_{22} of a thermal pulse from a He II-vapor interface is obtained by the direct measurement of the temperature rises of an incident and a reflected thermal pulses with the superconductive temperature sensor. It is confirmed that the experimental reflection coefficient R_{22} is about 0.8 except near the λ point. The present experimental result is found to agree quite well with the previous experimental results[21], [25], [33].

3. The experimental value of R_{22} is compared with the correct theoretical value of R_{22}. It is confirmed that the condensation coefficient of He II has the temperature dependence.

4. The value of R_{22} that is converted from the condensation coefficients obtained experimentally through the same estimation procedure of theoretical value R_{22} is derived. It is found that the agreement between the direct measurement result R_{22} and that converted from the condensation coefficient is fairy good. The satisfactory agreement between data obtained in the two independent measurements indicates the both measurements of α_c and R_{22} are valid.

5. The temperature amplitude reflection coefficient of a second sound from a rigid wall is measured with a wall mount type superconductive temperature sensor for the comparison with the reflection coefficient R_{22} from a He II free surface. It is found that the reflection coefficient $R_{22,rigid}$ from a rigid wall is unity.